Multi Morphological Sparse Regularized Image Super-Resolution Reconstruction Based on Machine Learning Algorithm

Jie Zhang, Jiali Tang, Xinling Feng

***Abstract*—The traditional image super-resolution (SR) reconstruction methods do not carry out sparse coding when performing SR reconstruction, resulting in poor structural similarity of image SR reconstruction. Therefore, this paper proposes a a super-resolution reconstruction method for polymorphic sparsity regularized images based on machine learning algorithms and builds a sparse representation model of polymorphic regularized images. For sparse representation models with different norm constraints, the orthogonal matching tracking in the greedy algorithm is used perform sparse coding to solve the sparse representation coefficient. The least square method in machine learning algorithm is used to solve the inverse operation of dictionary matrix update, construct the image super-resolution reconstruction minimization objective function, and solve the loss function between the super-resolution reconstruction image and the actual image, so as to complete the super-resolution reconstruction of polymorphic sparsity regularized image. The experimental results show that the edge recovery of the image under the proposed method is clearer, and the edge with more distinct edges and corners can be reconstructed. The Peak-Signal-to-Noise Ratio (PSNR) of the super-resolution reconstruction image is 60.5dB, and the Structural Similarity (SSIM) of the super-resolution reconstruction image is as high as 0.99, which effectively improves the image reconstruction effect.**

***Index Terms*—Super-resolution; Machine Learning; Sparse Coding, Least Square Method, Orthogonal Matching Tracking**

I. Introduction

Image is one of the main media for human to obtain information, and it has also become an important material for various analysis algorithms (such as image recognition, image classification, etc.) [1]. To obtain images with better visual effects and more additional information and details, there is a strong demand for high-resolution images in various fields. At present, as a research hotspot, image super-resolution reconstruction technology has been applied in many fields. In medical imaging, super-resolution reconstruction technology is used to process medical images obtained from CT imaging, X-ray imaging and nuclear magnetic resonance imaging, so as to provide doctors with high-resolution (HR) diagnostic media while reducing the radiation amount imposed on patients by imaging [2-3]. In terms of public security, although security monitoring has been popularized at present, it is difficult to obtain HR images or videos due to cost constraints. The use of image super-resolution reconstruction technology can improve its quality so that the next machine vision can find license plates or faces or supply clearer evidence for the police. In terms of military reconnaissance, small target detection of ships, vehicles, etc. or more detailed observation of target details can be achieved by super-resolution processing of remote sensing images taken by remote sensing satellites or reconnaissance aircraft [4, 5]. Because of the above advantages, super-resolution image reconstruction has become a promising choice. Under the original hardware conditions, it is an effective method to obtain HR images by using image SR reconstruction technology at low cost through software.

For this reason, relevant scholars have carried out a series of studies and made some progress. For example, Zhuang et al. proposed a regularized image super-resolution reconstruction method that improved the P2M framework [6]. They applied the residual network structure to image super-resolution reconstruction, using multiple small-scale convolution kernels instead of large-scale convolution kernels for training, so that the deep feature map can obtain a larger receptive field. They introduced an adaptive gradient clipping strategy, which can constrain the training gradient to a specific range through gradient clipping VDSR, The improved P2M framework is used to realize regularized image super-resolution reconstruction. This method can prevent the image gradient from disappearing, and the reconstruction effect is improved, but the PSNR of image super-resolution reconstruction is poor. Sun et al. applied a multi-scale feature fusion method to multi-modal sparse regularized image super-resolution reconstruction [7], used residual unit to obtain recursive blocks of regularized image, used information entropy method to calculate

Manuscript received December 07, 2022; revised April 09, 2023. This work was supported by Changzhou Sci&Tech Program (CE20215029).

Jie Zhang is a Senior Experimentalist at the School of Computer Engineering, Jiangsu University of Technology, Changzhou 213001, China.(corresponding author to provide phone:+86-519-86953240, fax: +86-519-86953240, e-mail: zhangjie@jsut.edu.cn).

Jiali Tang is a professor at the School of Computer Engineering, Jiangsu University of Technology, Changzhou 213001, China. (e-mail: tangjl@jsut.edu.cn).

Xinling Feng is a lecturer at the School of Computer Engineering, Jiangsu University of Technology, Changzhou 213001, China. (e-mail: fengxl@jsut.edu.cn).

residual block sharing weight, used multi-scale feature fusion method to achieve regularized image SR feature fusion, and achieved regularized image SR reconstruction based on back projection. This method can effectively improve the ability of image super-resolution feature information fusion, but the effect of image SR reconstruction is poor. Chen et al. used Convolutional Neural Networks (CNN) to conduct research on multi-modal sparse regularized image super-resolution reconstruction [8], used expanded convolutional layers to build image SR reconstruction trainers, used bit depth HDR mapping to match image features, and used depth learning methods to achieve image SR reconstruction. This method can improve the color restoration of images, but the image super-resolution reconstruction effect is poor.

To solve the above problems, this paper applies machine learning algorithm to image super-resolution reconstruction, uses the least square method of machine learning algorithm to solve the inverse operation of dictionary matrix update, constructs the minimum objective function of image SR reconstruction, and solves the loss function between the SR reconstruction image and the actual image to complete the multi-modal sparse regularized image SR reconstruction.

II. MULTI MORPHOLOGICAL REGULARIZED IMAGE SPARSE PROCESSING

A. Sparse representation model for multi morphological regularized images

Natural images are sparse in some transformation domains, that is, after some linear transformation of the image, most of the coefficients are zero [9]. Suppose $x_i \in R^m$ is the vector form of the i image block in image, and matrix $D \in R^{m \times n}$ is an over complete dictionary, where $m > n$, the image block can be approximately represented as:

$$x_i \approx Da_i \tag{1}$$

In formula (1), under dictionary D, the sparse representation coefficient of multimodal regularized image block x_i is represented by a_i, and the sparse representation process of multimodal regularized image is shown in Fig. 1.

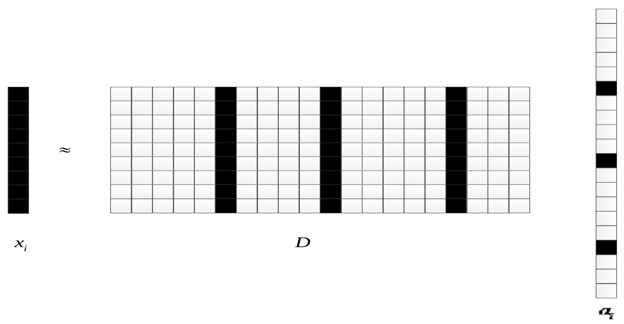

Fig. 1. Sparse representation model

To improve the super-resolution reconstruction effect of the multimodal regularized image, the sparse representation coefficient of the multimodal regularized image block is constructed by formula (2). The solution equation is:

$$a'_i = \min \|a_i\|_0 \quad s.t. \|x_i - D\alpha_i\|_2^2 \le \varepsilon \tag{2}$$

In formula (2), $\|\cdot\|_0$ represents the L_0 norm of image block feature vector, and ε represents the maximum allowable error of super resolution reconstruction sparse representation coefficient [10]. Therefore, L_1-norm is usually used to constrain the sparse representation coefficient. At this time, equation (2) can be converted into:

$$a'_i = \min \|a_i\|_1 \quad s.t. \|x_i - D\alpha_i\|_2^2 \le \varepsilon \tag{3}$$

With the help of Lagrangian multipliers, equation (3) is transformed into equation (4):

$$a'_i = \arg\min \|x_i - D\alpha_i\|_2^2 + \lambda \|\alpha_i\|_1 \tag{4}$$

Where, λ is the balance parameter. Equation (4) is the commonly used image sparse representation optimization equation, which is used to solve the sparse representation coefficient under the L_1-norm constraint.

B. Multimodality regularized image sparse coding

The sparse representation theory posits that any image can be sparsely represented under an appropriate overcomplete dictionary, where the majority of the representation coefficients are zero while only a few have large magnitudes. This sparse representation model of images can capture their inherent structure and prior properties. It has been widely applied in various inverse problems, such as image denoising, deblurring, source separation, and inpainting, and has achieved excellent experimental results. However, images are complex signals that contain various structural patterns, such as edges, contours, and textures. To form a sparse representation of images, a multi-component dictionary that matches the various structural patterns in the image should be constructed, and the sub-component dictionaries should be mutually incoherent, thereby forming a multi-modal sparse representation model of the image.

Greedy algorithm and relaxation algorithm are widely used for sparse representation models with different norm constraints. Greedy algorithm is to select the current local optimal solution in each optimization iteration to approximate the global optimal solution. OMP algorithm is widely used because of its simple principle and high sparse coding efficiency [11]. The solving process of orthogonal matching tracking for image block L_0 and dictionary $D = [d_1, d_2, ..., d_n]$ is as follows:

(1) Parameter assignment: residual $r^{(0)} = x_i$, image block a x tom set $D^{(0)} = \varnothing$, atom position index set $I^{(0)} = \varnothing$, error threshold ε, iteration number $k = 1$.

(2) Find the atom $d_n = \underset{dj \in D \setminus D^{(k-1)}}{\arg\max} \left| d_j, r^{(k-1)} \right|$ with the largest inner product of $r^{(k-1)}$ in the set $D \setminus D^{(k-1)}$, and return the position of the atom p.

(3) Update atomic set $D^{(k)} = D^{(k-1)} \cup d_p$ and index set $I^{(k)} = I^{(0)} \cup p$.

(4) Use the least squares method to calculate the representation coefficient of the image block under $D^{(k)}$ [12]:

$$\alpha_i^{(k)} = \arg\min \|x_i - D^{(k)} \alpha_i\|_2 \tag{5}$$

(5) Update residual $r^{(k)} = x_i - D^{(k)}\alpha_i^{(k)}$.

(6) Judge whether the residual error is less than the threshold value. If it is satisfied, stop the iteration. Output the sparse representation coefficient according to $I^{(k)}$ and $\alpha_i^{(k)}$. If it is not satisfied, return to step (2) and update the iteration number $k = k+1$.

The relaxation algorithm is mainly used to perform convex relaxation for non-convex L_0-norm optimization problems, and then the final solution can be obtained by solving the corresponding programming problem. BP algorithm transforms the minimization problem with L_0-norm constraint into a L_1-norm constraint, i.e. the sparse representation model shown in equation (3), and then converts it into a linear programming problem for optimal solution. The GP algorithm transforms the L_1-norm problem into a boundary constrained quadratic programming problem, and then uses the gradient projection to perform iterative optimization.

Another important factor that affects the image sparse representation effect is the selection of sparse dictionaries. Different dictionaries have different image feature information. According to different acquisition methods, dictionaries can be divided into fixed dictionaries and learning dictionaries. The corresponding fixed dictionary can be constructed by using the sparsity of the image under a fixed transformation basis [13]. This type of dictionary construction method is relatively simple, and the algorithm implementation speed is relatively fast. However, when the structure information in the image is relatively complex, it is difficult for fixed dictionaries to effectively sparse decompose all geometric structures, resulting in poor image sparse representation. In addition, because the construction method is determined, it lacks adaptability for different types of images, and is difficult to meet different application requirements.

Another kind of dictionary construction method is to use a large number of sample image blocks for dictionary training, and learn from them to obtain an over complete dictionary with good sparse representation effect [14]. Compared with the traditional fixed dictionary, the dictionary obtained through sample learning has strong adaptability. The dictionary contains rich image feature information, which can meet the sparse representation requirements of different types of structures in the image. During the construction of a learning dictionary, L_0 norm is usually used to constrain the sparse property. At this time, the mathematical model of dictionary learning can be expressed as:

$$\min_{D,\alpha} \|x - D\alpha\|_F^2 \ s.t. \|\alpha_i\|_0 \le T_0 \tag{6}$$

Wherein, $\alpha = [\alpha_1, \alpha_2, ..., \alpha_N]$ is the sparse representation coefficient matrix of the training image block, T_0 is the sparsity.

For the solution of the problem shown in equation (6), the optimal method algorithm realizes the dictionary learning process through the alternate iteration of sparse representation coefficient and dictionary [15]. When the dictionary is determined, equation (6) is transformed into:

$$\min_{\alpha} \|x - D\alpha\|_F^2 \ s.t. \|\alpha_i\|_0 \le T_0 \tag{7}$$

When the sparse representation coefficient is known, the mathematical model of dictionary learning in equation (6) is transformed into:

$$\min_{D} \|x - D\alpha\|_F^2 \tag{8}$$

Equation (8) shows the least squares problem, which can be solved by the following equation:

$$D' = x\alpha^{\mathrm{T}}(\alpha \cdot \alpha^{\mathrm{T}})^{-1} \tag{9}$$

Wherein, T represents the transposition. Because equation (9) needs to calculate the inverse of the matrix when updating the dictionary, the computational complexity of the algorithm is increased. At this point, the multi morphological regularized image sparse coding is completed.

III. Super-resolution Reconstruction of Multi Morphological Regularized Images Based on Machine Learning

A. Design of minimum objective function based on machine learning

In recent years, the super-resolution research method based on machine learning has developed rapidly, mainly by collecting a large number of pictures, establishing a sample library of learning models, using different machine learning methods to learn the relationship between high and low resolutions through a large number of model training, and then by adjusting the parameters to enlarge the image to the required size, while capturing and restoring the details in the image [16]. Compared with the interpolation calculation method and the calculation method used to reconstruct an image, the machine learning reconstruction algorithm needs more computing power to accurately depict the overall high-dimensional structural features of an image and more accurate computing power for abstract reproduction of image structural details [17]. The main steps of training model are as follows.

(1) The original image is degraded, and image processing methods such as clipping, flipping and affine are used to expand the dataset to make the learning samples more sufficient.

(2) The different regions of the original image are divided into blocks to separate the high-frequency information region and low-frequency information region in the image, and then the algorithm is used to learn the image features and accumulate prior knowledge, and a proper learning model is constructed to fit the real information.

(3) According to the high-frequency information in the low resolution image, the high-frequency image with the highest matching degree is found in the training sample library.

Traditional super-resolution reconstruction algorithms based on convolutional neural networks mostly use Mean Squared Error (MSE) as the objective function to be minimized. While using MSE as the objective function can achieve a high peak signal-to-noise ratio in the reconstructed image, when the magnification factor is high, the reconstructed image may be too smooth and lose details, resulting in poor subjective quality.

The design process of minimizing the objective reconstruction function based on machine learning algorithm is given below [18].

Formula (10) stands for the objective function of the sparse representation algorithm in the super-resolution reconstruction algorithm based on machine learning:

$$\theta' = \min_{\theta} \|\partial\|_1 + \frac{1}{2}\|\overline{D}\partial - \overline{y}\|_2^2 \qquad (10)$$

In formula (10), $x_i \in R_i$ is used to describe the i image block in the LR image, $y_i \in R_m$ is used to describe the corresponding HR image feature block, and ∂ is the sparse representation coefficient of the image reconstruction function, which is between 0 and 1.

$$\overline{D} = \begin{bmatrix} FD_1 \\ FD_k \end{bmatrix}, \overline{y} = \begin{bmatrix} Fy \\ w \end{bmatrix} \qquad (11)$$

In the formula, F represents the feature extraction operator, and w represents the pixel in the reconstructed HR region. If D_k is an overcomplete dictionary in the reconstruction process, the objective function of minimizing sparse representation can be simplified as follows.

$$x_i \approx D_h \partial \qquad (12)$$

Fig. 2 shows the process of machine learning multimodal regularized image super-resolution reconstruction. First, the HR image set is degraded to generate an LR image set, and then the LR image set is interpolated and magnified to the size required for super-resolution reconstruction. Then, the magnified interpolation image is divided into LR feature set blocks, and the magnified interpolation image is subtracted from the HR image set to obtain the HR feature set block, Finally, LR feature set block and HR feature set block are used as input, and LR dictionary and HR dictionary are obtained through training. The above is the dictionary construction part. The sparse coefficient solution part is to interpolate and enlarge the LR image to be reconstructed to obtain the LR feature cluster, and build the sparse representation of image reconstruction together with LR. Then add the bicubic interpolated image and the corresponding sparse representation to obtain HR image blocks, and then splice these HR image blocks to obtain HR images. This method has many practical applications, but it also has the problem of solving instability.

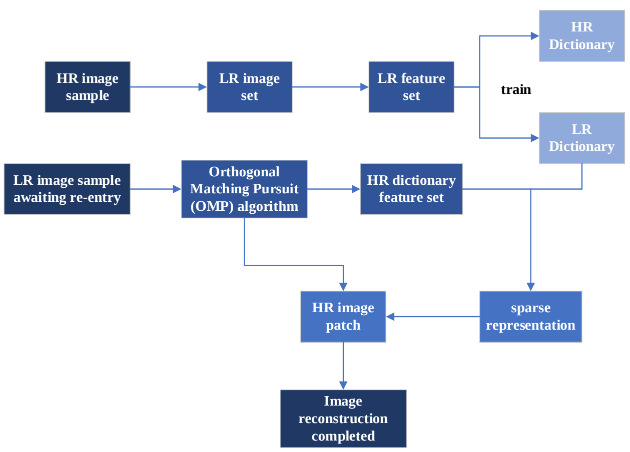

Fig. 2. Multimodality sparse regularized image SR reconstruction process

B. Image super-resolution reconstruction

Based on Fig. 2, the image super-resolution reconstruction algorithm is implemented. First, given that the input LR image is I_{LR}, the HR image before degradation is I_{LR}. Then the image degradation model is:

$$I_{LR} = \Psi(I_{HR}, \delta) \qquad (13)$$

Among them, Ψ represents the image degradation function (degradation function is generally set manually according to experience or obtained through learning), and δ represents the degradation parameter. In the image super-resolution reconstruction algorithm, δ is generally noise and scale factor. If the high-resolution image reconstructed by the algorithm is I_{SR}, the reconstruction model is expressed as:

$$I_{SR} = \xi(I_{HR}, \theta) \qquad (14)$$

Among them, ξ is the reconstruction algorithm model, and θ is the model parameter. The gap between I_{SR} and I_{HR} is reduced by constantly adjusting the model parameters. In reality, degradation function Ψ is affected by many factors (such as environmental noise, camera distortion, compression artifacts, sensor noise, etc.). To better fit the degradation model of the real world, SRMD network models the degradation process more specifically as:

$$\Psi(I_{HR};\delta) = (I_{HR} \otimes \kappa)\downarrow_s + n_{\varsigma}, \{\kappa, s, \zeta\} \subset \delta \qquad (15)$$

Among them, $I_{HR} \otimes \kappa$ represents the convolution between the fuzzy kernel κ and the HR image to simulate the image blur process, $\downarrow_s$ represents the image down sampling operation to simulate the process of image resolution loss, and n_{ς} represents the white noise conforming to the standard deviation Gaussian distribution to simulate the noise in the environment.

Although this model is more in line with the process of image degradation in reality, it is difficult to design algorithms based on this model. In addition, the environment noise is complex, so the algorithm spends most of its performance learning the changes of environment noise, but has little benefit. Therefore, in order to simplify the model design, most of the work will simplify the degraded model:

$$\Psi(I_{HR};\delta) = (I_{HR})\downarrow_s, \{s\} \subset \delta \qquad (16)$$

The down sampling process of scale factor s generally uses double cubic down sampling. Reduce the gap θ' between the reconstructed image I'_{SR} and the real image I_{HR}:

$$\theta' = \arg\min_{\theta} \Psi(I'_{SR}, I_{HR}) \qquad (17)$$

The loss function between the real image and the super resolution reconstructed image is described by $\Psi(I'_{SR}, I_{HR})$. At this time, the value of the minimum loss function obtained is θ', which is the super-resolution image reconstruction effect of the super-resolution reconstruction image. Therefore, the multi-modal sparse regularization image super-resolution reconstruction is completed.

IV. Experiment and Discussion

A. Experimental Design

The experimental platform is equipped with 12GB computer memory. To ensure the realization of functions, GTX1080Ti GPU graphics card is selected when configuring hardware. Matlab is used for data preprocessing, Jupyter is used for model construction and training, and TensorFlow is used as the software platform of the deep neural network framework. This software is a commonly used deep learning framework at this stage, with the advantages of strong code readability and simple operation. It is used to train the model parameters. The validation set and testing set are composed of another 200 pictures in equal proportions, respectively, to evaluate the model quality and generalization ability in the training process. They have rich details in different frequency bands. Manga109 is composed of images taken from Japanese cartoons. These images are computer generated and have different characteristics from natural images.

This paper uses the experimental training dataset of DIV2K image set. In order to facilitate the comparison experiment, Set5, Set14 and BSD100 datasets, which are commonly used at present, are selected for testing. Before starting the model training, the experimental data shall be preprocessed, and the image processing technology shall be used to analyze the LR image data samples to be used in the experiment. The actual data preprocessing procedure is shown in Fig. 3.

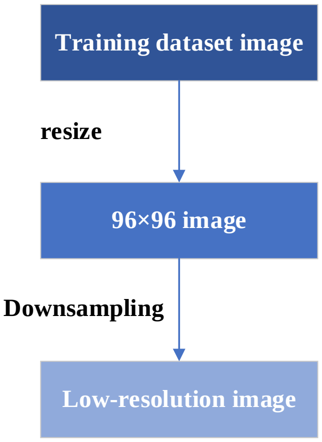

Fig. 3. Schematic diagram of data preprocessing procedure

Because the image size of the image dataset is inconsistent, the original HR image should be preprocessed before training. The first step is to cut the training image data used in the experiment to make it become a small size image block, as shown in Fig. 3. The actual process is to use Matlab to edit the cutting program, and then cut the image through the 96*96 sliding window to process the image into 96*96 pieces. The obtained images are processed by double cubic interpolation down sampling and up sampling, and finally the image sets with magnification factors of 2 times, 3 times and 4 times are obtained, so as to obtain LR image data samples through HR image data samples.

B. Evaluation index of reconstructed image quality

The quality evaluation of the reconstructed image is an indispensable step in super-resolution reconstruction, and efficient evaluation criteria can quickly and accurately know the reconstruction effect. Evaluation is divided into subjective evaluation and objective evaluation.

(1)Subjective evaluation method

The subjective quality evaluation method is mainly to evaluate the sharpness of the reconstructed image according to each person's subjective feeling and the similarity between the reconstructed image and the original image. The score generally fluctuates between 1 (poor quality) and 5 (good quality). The score of each test is recorded as c_i, and the total number of people evaluated is recorded as n_i, so the mean value of the sensory score of each image is MOS:

$$MOS = \frac{\sum_{i=1}^{k} c_i n_i}{\sum_{i=1}^{k} n_i} \tag{18}$$

The subjective evaluation method generally refers to the qualitative analysis of the effect of the reconstructed image from everyone's visual angle, that is, the overall effect of the reconstructed image, which can be evaluated more realistically. The difference between the observers and the observation times will lead to a large difference in the evaluation results, and the difference in the observation environment will also lead to the difference in the evaluation results. If the difference between images is very small, it will affect the accuracy and accuracy of the assessed visual perception. The subjective evaluation process cannot be accurately quantified, resulting in a certain degree of unilateralism.

(2) Objective evaluation method

The objective evaluation is to evaluate the quality of images from a mathematical point of view. It is highly objective, and the evaluation results can also be reproduced. After the evaluation model is encapsulated, the images can be evaluated in batches. The specific method is to compare the pixel points of the reconstructed image with the original image one by one to obtain the difference between them.

① PSNR

$$PSNR = 10 * \log_{10} \frac{MAX^2}{MSE} = 20 * \log_{10} MAX_1 - 10 * \log_{10} MSE \tag{19}$$

Among them, MAX stands for the gray peak value of the multimodal sparse regularized image, and MSE represents the mean square error.

② SSIM

There may be a strong correlation between the neighborhood of an image and two adjacent pixels, but PSNR only considers the pixel difference between the reconstructed image and the original image, and does not consider the correlation in each pixel field of the image. SSIM is expressed by formula (20):

$$SSIM(x,y) = [l(x,y)]^{\alpha}[c(x,y)]^{\beta}[s(x,y)]^{\gamma} \tag{20}$$

Wherein, x stands for the tested image and y represents the actual image. Use $l(x,y)$ to describe the brightness function of the multimodal regularized image, $c(x,y)$ to describe the contrast function of the multimodal regularized image, and $s(x,y)$ to describe the structure term function of the multimodal regularized image. The calculation process is shown in formula (21) to (23):

$$l(x,y)=\frac{2\mu_x\mu_y+C_1}{\mu_x{}^2+\mu_y{}^2+C_1} \tag{21}$$

$$c(x,y)=\frac{2\sigma_x\sigma_y+C_2}{\sigma^2{}_x+\sigma^2{}_y+C_2} \tag{22}$$

$$s(x,y)=\frac{2\sigma_{xy}+C_2}{\sigma^2{}_x+\sigma^2{}_y+C_2} \tag{23}$$

In the above formula, μ_x represents the average value of pixels of the multi morphological sparse regularized image, μ_y represents the average value of the original image, $\sigma^2{}_x$ represents the variance of the multi morphological sparse regularized reconstructed image, $\sigma^2{}_y$ represents the variance of the high-definition image, and σ_{xy} represents the covariance of the original high-definition image and the reconstructed image. C_1 and C_2 represent constant terms in the function, which is mainly used to prevent the denominator of these three functions from being zero:

$$SSIM(x,y)=\frac{(2\mu_x\mu_y+C_1)(2\sigma_{xy}+C_2)}{(\mu_x{}^2+\mu_y{}^2+C_1)(\sigma^2{}_x+\sigma^2{}_y+C_2)} \tag{24}$$

According to the above process, complete the calculation of structural similarity results, and conduct the following experimental verification.

C. Experimental Result

1) Image reconstruction effect (MOS)

To verify the effect of image super-resolution reconstruction, the method in reference [6], the method in reference [7] and the effect of image SR reconstruction under the method of this paper are counted, and the results are shown in Fig. 4 and 5.

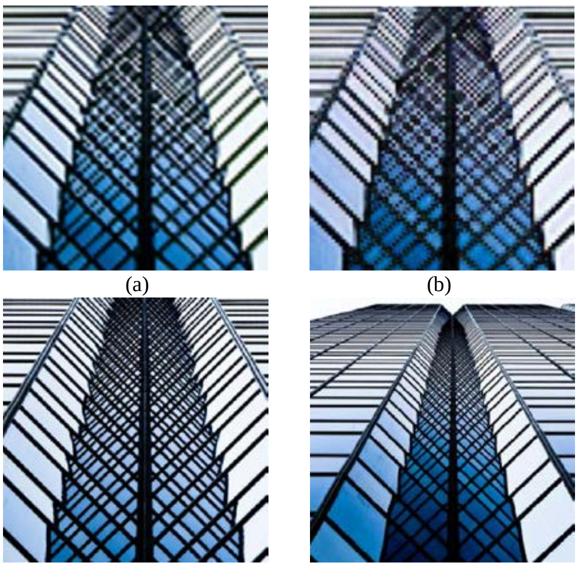

(a) (b) (c) (d)

Fig. 4. SR reconstruction of building images
(a) Method in Ref. [6]; (b) Method in Ref. [7]; (c) Our method; (d) Original image

It can be seen from Fig. 4 and 5 that the reference [6] method and reference [7] method in the reconstruction picture have produced obvious noise, and the picture seems to have many spots; The method in this paper can restore the edges of buildings more clearly, and reconstruct the edges with more distinct edges and corners. Through comparative experiments, it is verified that the algorithm proposed in this study can better reconstruct multi morphological sparse regularized images.

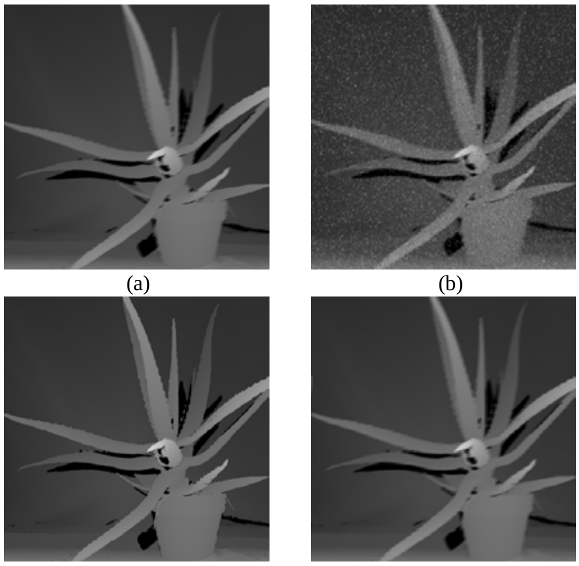

(a) (b) (c) (d)

Fig. 5. SR reconstruction effect of green plant image
(a) Method in Ref. [6]; (b) Method in Ref. [7]; (c) Our method; (d) original image

2) PSNR of Image Super Resolution Reconstruction

To verify the image super-resolution reconstruction effect of the method in this paper, the method in reference [6], the method in reference [7] and the PSNR of image SR reconstruction under the method in this paper are counted, and the results are shown in Table I.

TABLE I
PSNR OF IMAGE SUPER RESOLUTION RECONSTRUCTION

Number of images/piece	PSNR of Image SR Reconstruction/dB		
	Method in Ref. [6]	Method in Ref. [7]	Our method
500	28.9	32.1	66.5
1000	32.8	28.3	68.2
1500	38.6	33.6	63.1
2000	30.1	38.9	60.5
2500	29.8	29.0	69.2
3000	28.3	35.2	70.3

Table Ⅰ shows that the PSNR of image SR reconstruction under different methods is different. When the number of images is 500, the PSNR of the super-resolution reconstruction image in reference [6] method is 28.9dB, in reference [7] method is 32.1dB, and in our method is 66.5dB; When the number of images is 1000, the PSNR of the super-resolution reconstruction image in reference [6] method is 32.8dB, in reference [7] method is 28.3dB, and in our method is 68.2dB; When the number of images is 2000, the PSNR of the super-resolution reconstruction image in reference [6] method is 30.1dB, in reference [7] method is 38.9dB, and in our method is 60.5dB. The PSNR of the SR reconstruction image in our method is far higher than other methods, which shows that it can improve the image reconstruction effect.

3) SSIM of image super-resolution reconstruction

To verify the effect of multi-modal sparse regularized image super-resolution reconstruction, the method of reference [6], the method of reference [7] and the structural similarity of image SR reconstruction under the method of this paper are counted, and the results are shown in Fig. 6.

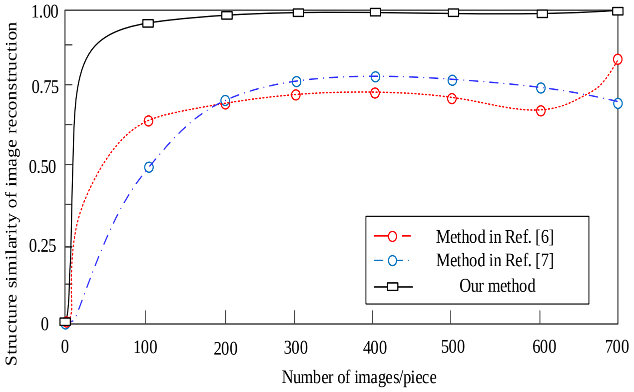

Fig. 6. SSIM of image super-resolution reconstruction

It can be seen from the analysis of Fig. 6 that when the number of images is 100, the SSIM of image super-resolution reconstruction in reference [6] method is 0.63, in reference [7] method is 0.48, and in our method is 0.91; When the number of images is 500, the structural similarity of image super-resolution reconstruction in reference [6] is 0.70, in reference [7] is 0.73, and in our method is as high as 0.99. The above results show that the image SR reconstruction SSIM of this method is the highest, indicating that this method has a positive role in image reconstruction.

4) Verification of image super-resolution reconstruction efficiency

To analyze the efficiency of super-resolution reconstruction of morphological sparse regularized images, this paper will make statistics on the method of reference [6], the method of reference [7] and the time consumption of SR reconstruction of morphological sparse regularized images. The specific experimental results are shown in Table II.

TABLE Ⅱ
IMAGE SUPER-RESOLUTION RECONSTRUCTION EFFICIENCY

Number of image reconstruction samples/piece	Time consuming for image SR reconstruction/s		
	Method in Ref. [6]	Method in Ref. [7]	Our method
1000	132.8	128.3	8.1
2000	286.5	225.8	10.6
3000	396.0	482.9	13.2
4000	568.2	688.1	15.9
5000	862.9	982.5	18.3
6000	998.1	1223.2	20.5

Analysis of Table II shows that when the number of image reconstruction samples is 1000, the image super-resolution reconstruction time in reference [6] method is 132.8s, in reference [7] method is 128.3s, and in the method proposed in the paper is 8.1s; When the number of image reconstruction samples is 3000, the image super-resolution reconstruction time in reference [6] method is 396.0s, in reference [7] method is 482.9s, and in the method proposed in the paper is 13.2s; When the number of image reconstruction samples is 6000, the image super-resolution reconstruction time in reference [6] method is 998.10s, in reference [7] method is 1223.2s, and in the method proposed in the paper is 20.5s. The time consumption of image super-resolution reconstruction under this method is always low, which reflects that the efficiency of our method in image SR reconstruction has been improved.

V. CONCLUSION

In this paper, a multi morphological sparse regularized image super-resolution reconstruction method based on machine learning algorithm is proposed. The least square method in the machine learning algorithm is used to solve the inverse operation of dictionary matrix updating, and the minimization objective function of image super-resolution reconstruction is constructed to achieve the multi-modal sparse regularized image SR reconstruction. The experimental results show that:

(1) This method can restore the edges of buildings more clearly, and can reconstruct the edges with more distinct edges and corners. Through comparative experiments, it is verified that the algorithm proposed in this study can better reconstruct multi morphological sparse regularized images.

(2) When the number of images is 2000, the PSNR of the super-resolution reconstruction image in this method is 60.5dB, which shows that the method can improve the image reconstruction effect better.

(3) When the number of images is 500, the SSIM of the super-resolution image reconstruction of this method is as high as 0.99, which shows that this method plays a positive role in image reconstruction.

(4) In this paper, a sparse representation model of multimodal regularized images is built, and the sparse representation coefficients of multimodal regularized images by using orthogonal matching pursuit is solved, the inherent characteristics of multimodal regularized images is determined. The method improves the efficiency of image super-resolution reconstruction of this method. Under 6000 samples, the time consumption is only 20.5s.

REFERENCES

[1] A. W. Rosyadi, N. Suciati, "Image segmentation using transition region and K-Means clustering," IAENG International Journal of Computer Science, vol.47, no.1, pp47-55, 2020.

[2] P. Tian, L. Q. Cui, Y. X. Wang, L. Qin, J. M. Qin, "ECT Image Reconstruction Method Based on Improved Drosophila Optimization Algorithm," Journal of Sensing Technology, vol. 34, no. 12, pp. 1631–1637, 2021.

[3] X. H. Chen, J. S. Wang, Y. L. Ruan, S. Z. Gao, "An Improved Iris Recognition Method Based on Discrete Cosine Transform and Gabor Wavelet Transform Algorithm," Engineering Letters, vol. 27, no. 4, pp. 676-685, 2019.

[4] M. Liang, H. R. Wang, Y. Zhang, J. Li, "Image super resolution reconstruction method based on accelerated residual network," Computer Application, vol. 41, no. 5, pp. 1438–1444, 2021.

[5] X. Li, R. G. Ma, Y. X. He, "Backlit image reconstruction method based on sequence aperture photography," Computer Technology and Development, vol. 32, no. 6, pp. 79–84, 2022.

[6] Y. F. Zhuang, W. G. Wan, "3D Reconstruction of Single Image Based on P2M Framework Improvement," Electronic Measurement Technology, vol. 43, no. 9, pp. 61–64, 2020.

[7] C. W. Sun, X. Chen, "Image super resolution reconstruction based

on multi-scale feature fusion back projection network," Acta Automatica Sinica, vol. 47, no. 7, pp. 1689–1700, 2021.
[8] W. Chen, Q. Wang, "Research on the method of reconstructing HDR image from LDR image based on convolutional neural network," Packaging Engineering, vol. 41, no. 5, pp. 228–234, 2020.
[9] N. Li, S. L. Niu, "High precision SAR image water area segmentation method based on local super-resolution reconstruction," Journal of Radar Science, vol. 9, no. 1, pp. 174–184, 2020.
[10] Z. X. Wang, H. Q. Wang, Y. Zhang, "Photoacoustic tomography image reconstruction method based on TR interpolation algorithm," Foreign Electronic Measurement Technology, vol. 40, no. 4, pp. 1–5, 2021.
[11] L. P. Lin, H. M. Zhou, N. Ouyang, "A compressed perceptual image reconstruction method combining spatial position and structure information," Computer Application, vol. 42, no. 3, pp. 930–937, 2022.
[12] Y. Zhou, M. X. Chang, H. Ye, Y. Zhang, "Super resolution reconstruction method of defect image of solar panel based on meta migration," Computer Science, vol. 49, no. 3, pp. 185–191, 2022.
[13] B. H. Qiang, Y. C. Pang, M. H. Yang, K. Zeng, H. Zheng, W. Xie, Y. Mo, "Image super resolution reconstruction method based on embeddable network structure，" Computer Engineering, vol. 47, no. 5, pp. 221–228, 2021.
[14] Y. Q. Wang, X. Li, Y. Y. Fan, Y. R. Qian, "Single image super-resolution reconstruction based on feedback generation countermeasure network，" Computer Engineering and Design, vol. 43, no. 7, pp. 2022–2030, 2022.
[15] H. X. Wu, Z. Zhang, "3D image reconstruction method based on absolute conic image," Computer Simulation, vol. 38, no. 8, pp. 203–206+211, 2021.
[16] D. Zhao, L. Z. Zhao, Y. J. Gan, B. Y. Qin, "A magnetic resonance image reconstruction method without pre training based on supporting prior and depth image prior," Journal of Physics, vol. 71, no. 5, pp. 350–362, 2022.
[17] J. Liu, W. S. Wu, "Automatic Image Annotation Using Improved Wasserstein Generative Adversarial Networks," IAENG International Journal of Computer Science, vol. 48, no.3, pp507-513, 2021.
[18] J. Zhang, X. Liu, "Super resolution reconstruction of visual sensing image based on single-layer wavelet transform," Journal of Sensing Technology, vol. 35, no. 1, pp. 122–126, 2022.